

# The treatment of diffusion in the FRANEC CODE

(Degl’Innocenti, Prada Moroni, Marconi, Ruoppo)

**Diffusion of He and heavy elements.** The diffusion of the following heavy elements is explicitly calculated:  $^{12}\text{C}$ ,  $^{14}\text{N}$ ,  $^{16}\text{O}$ ,  $^6\text{Li}$ ,  $^7\text{Li}$ ,  $^9\text{B}$ ,  $^{11}\text{B}$ ,  $^{56}\text{Fe}$ . All the other heavy elements are assumed to diffuse as  $^{56}\text{Fe}$ . Electron diffusion is included.

**Diffusion coefficients** by Thoul et al. (1994) obtained as the solutions of the Burgers equations for a multi-components fluid, including the gravity (pressure), temperature and composition terms.

The rate of change of the element mass fractions due to diffusion is written in dimensionless form as:

$$\frac{\partial X_m}{\partial t} = -\frac{1}{\rho r^2} \frac{\partial [r^2 X_m T^{\frac{5}{2}} \xi_m(r)]}{\partial r} \quad (1)$$

where  $\xi_m(r)$  are the so called “diffusion functions” which (for each element m) are calculated as:

$$\begin{aligned} \xi(m) = & a_P(m) \frac{\partial \ln P}{\partial r} + a_T(m) \frac{\partial \ln T}{\partial r} + \sum_n a_X(m, n) \frac{\partial \ln X(n)}{\partial r} + \\ & - \sum_n a_X(m, n) \frac{\sum_j \frac{Z(j) X(j)}{A(j)} \frac{\partial \ln X(j)}{\partial r}}{\sum_i \frac{Z(i) X(i)}{A(i)}} \end{aligned} \quad (2)$$

where n is different from 2 (He) and 10 (electrons) but the sums over i and j are over all the ionic species taken into account.

The diffusion velocity is progressively reduced as the surface is approached (to reach a zero velocity at the surface). Radiative acceleration not included. The variation of the total metallicity, due to diffusion, is taken into account in the opacity calculation but not in the calculation of the EOS.

### Test of the diffusion efficiency with a standard solar model (SSM)

- Our SSM reproduces the helioseismological observables included the sound speed in the solar interior.

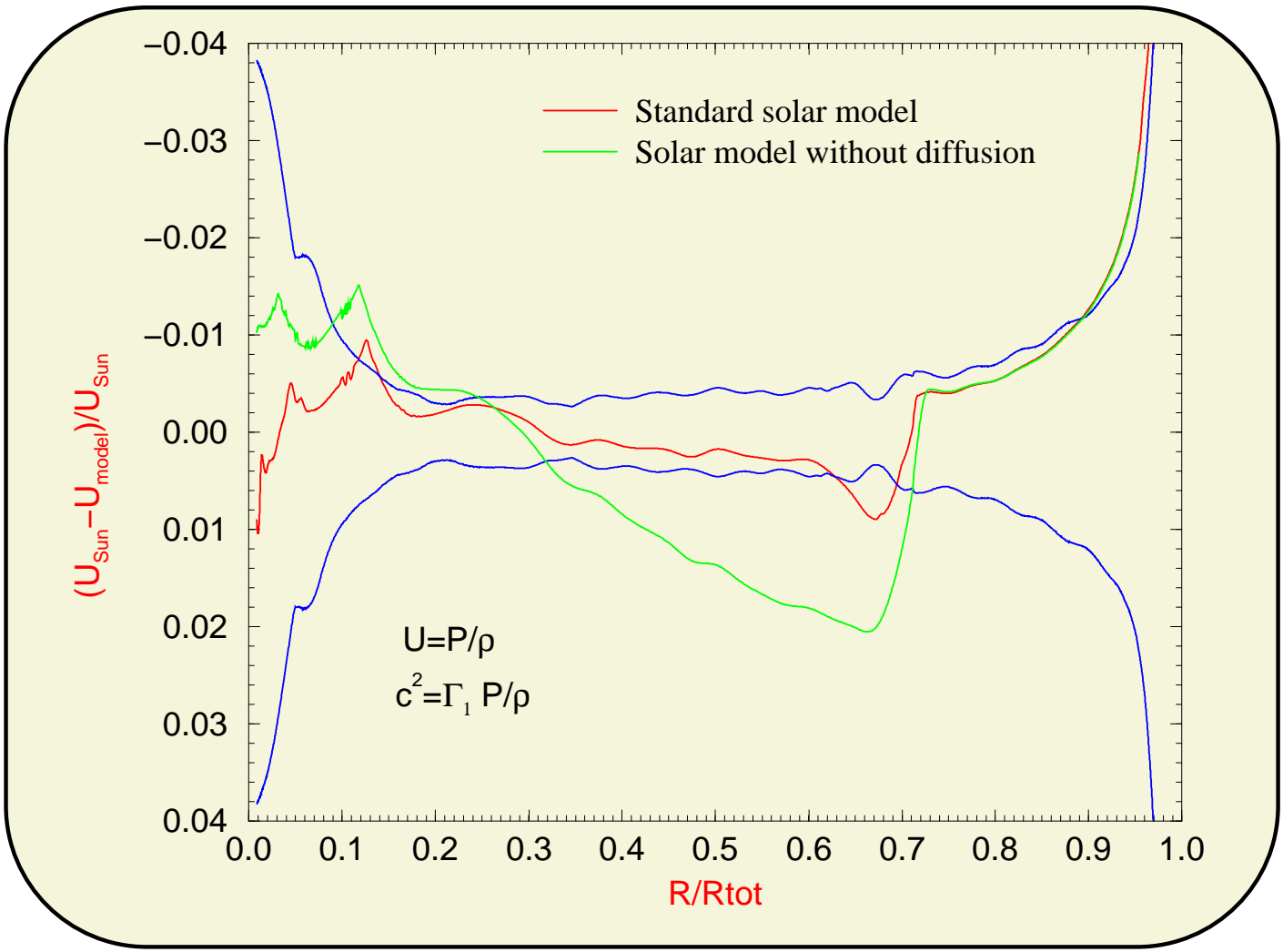


**Figure 1 :** Relative difference between the helioseismological sound speed and the result of our model. The region between the blue lines indicates the allowed region taking into account the uncertainties on the helioseismological results (Degl'Innocenti et al. 1997). The solar model has been calculated with the Grevesse & Noels (1993) composition.

## Effects of diffusion on the evolution of Population II stars

Evolution of a model with  $M=0.8 M_{\odot}$  without diffusion (ND), with He diffusion only (M1), with He and heavy metals diffusion (M2).

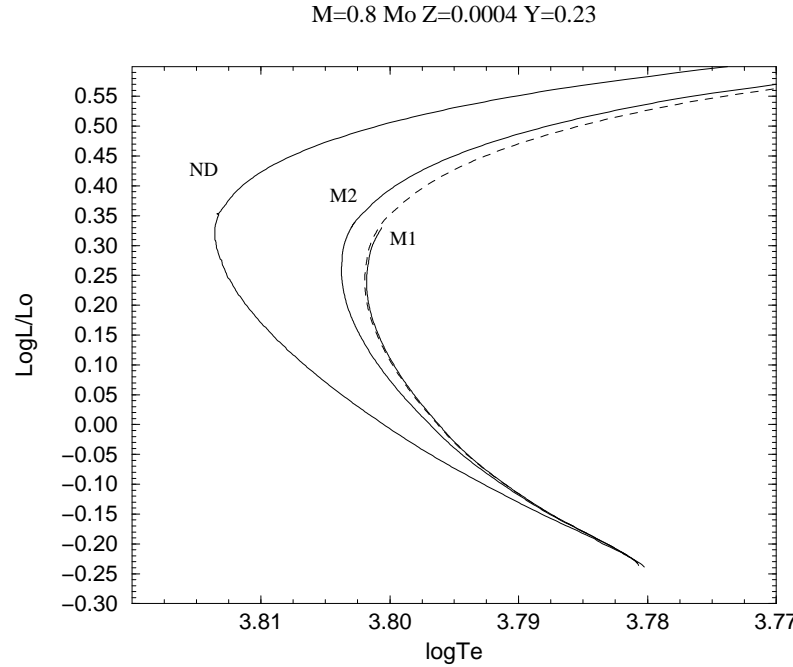


**Figure 2 :** Castellani, Ciacio, Degl'Innocenti, Fiorentini 1997, A&A 322, 801

Effect of diffusion on the TO absolute visual magnitude

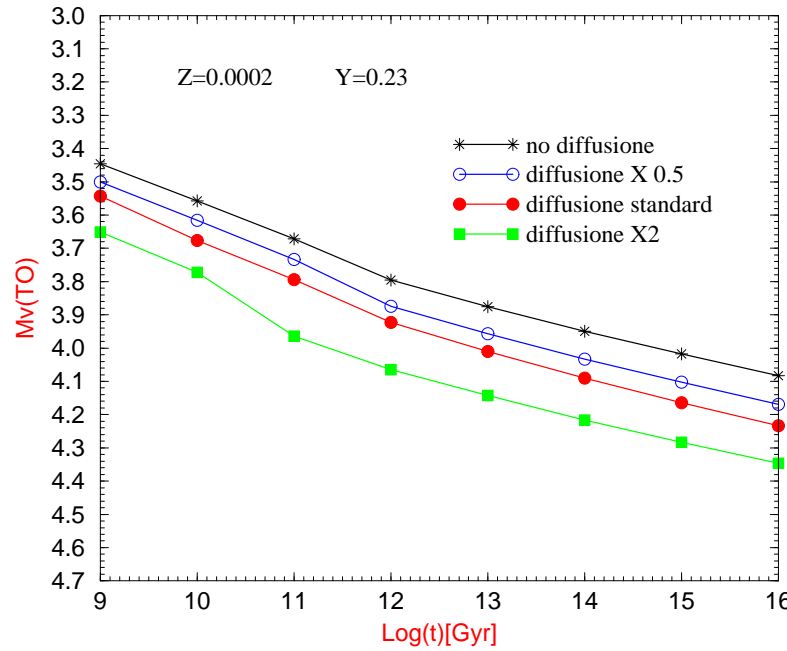
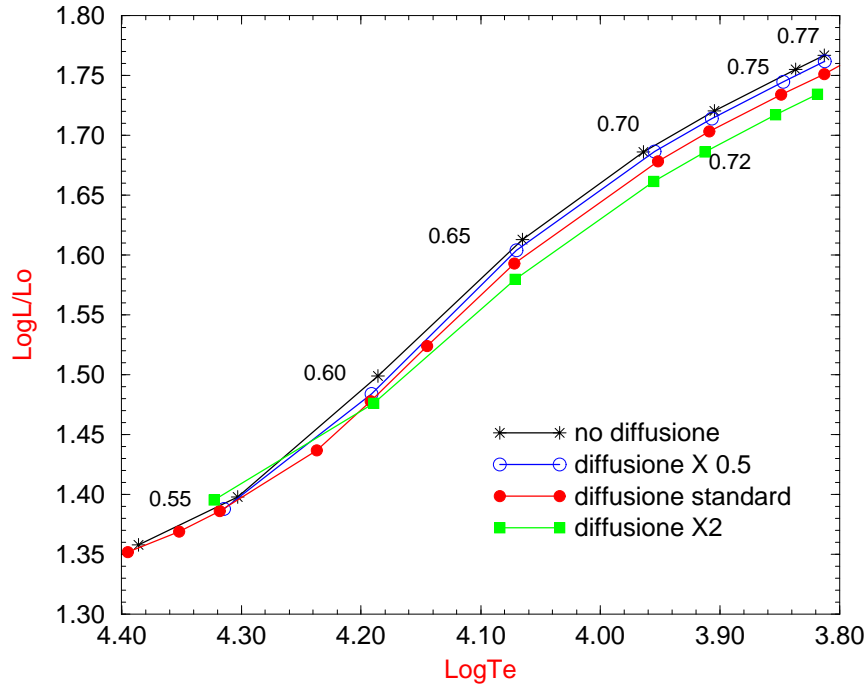


**Figure 3 :** Castellani, Degl'Innocenti 1999, A&A 344, 97

## ZAHB luminosity for different diffusion efficiencies



## $\Delta V_{\text{HB}}^{\text{TO}}$ for different diffusion efficiencies

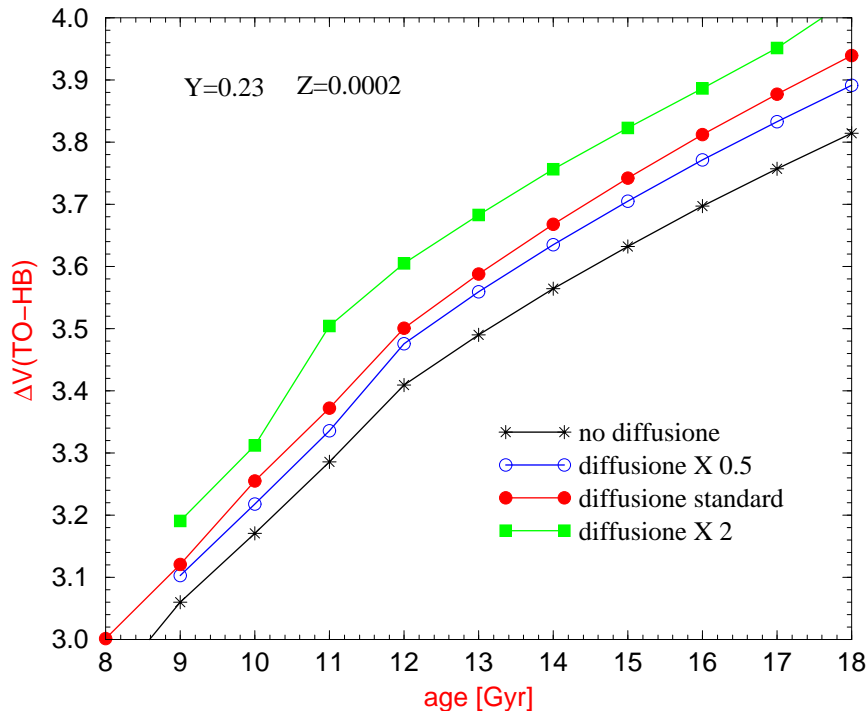


**Figure 4 :** Castellani, Degl'Innocenti 1999, A&A 344, 97

Updated models with microscopic diffusion nicely reproduce the CMD of galactic globular clusters

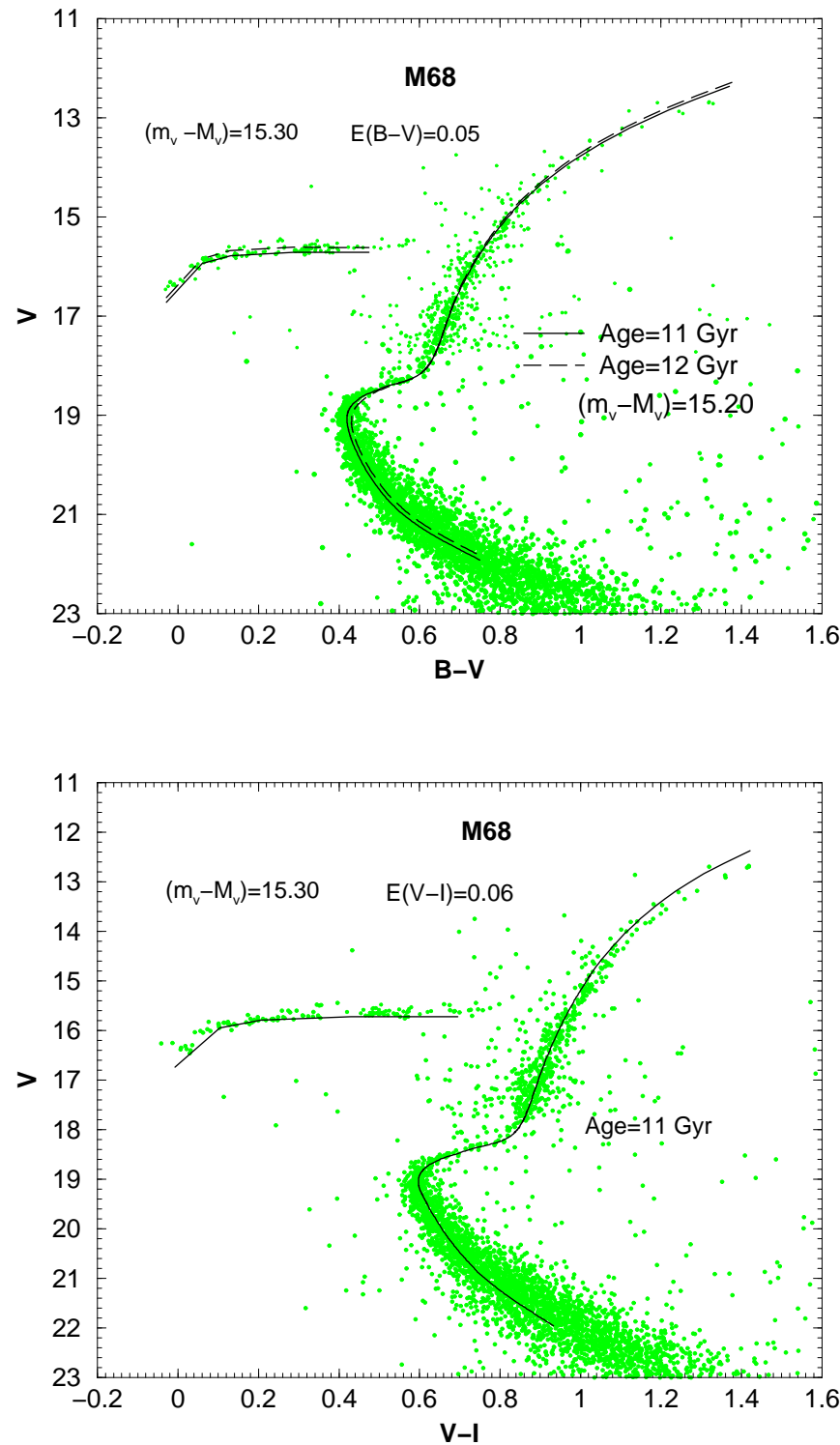


**Figure 5 :** Cariulo, Degl'Innocenti, Castellani, 2004, A&A 421, 1121

## Surface $^7\text{Li}$ abundance for PMS-MS models with microscopic diffusion

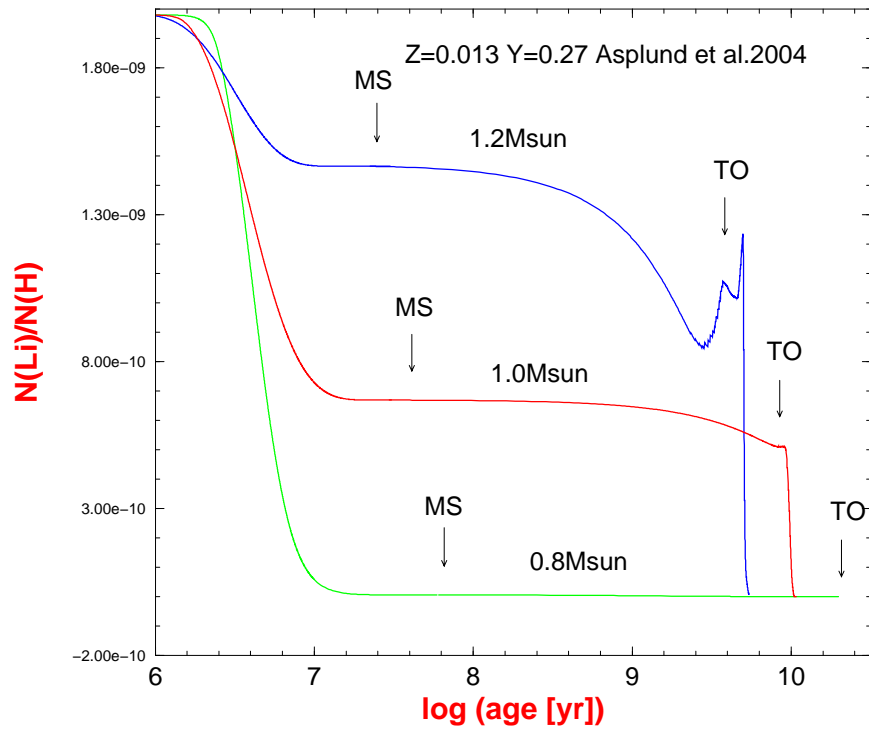
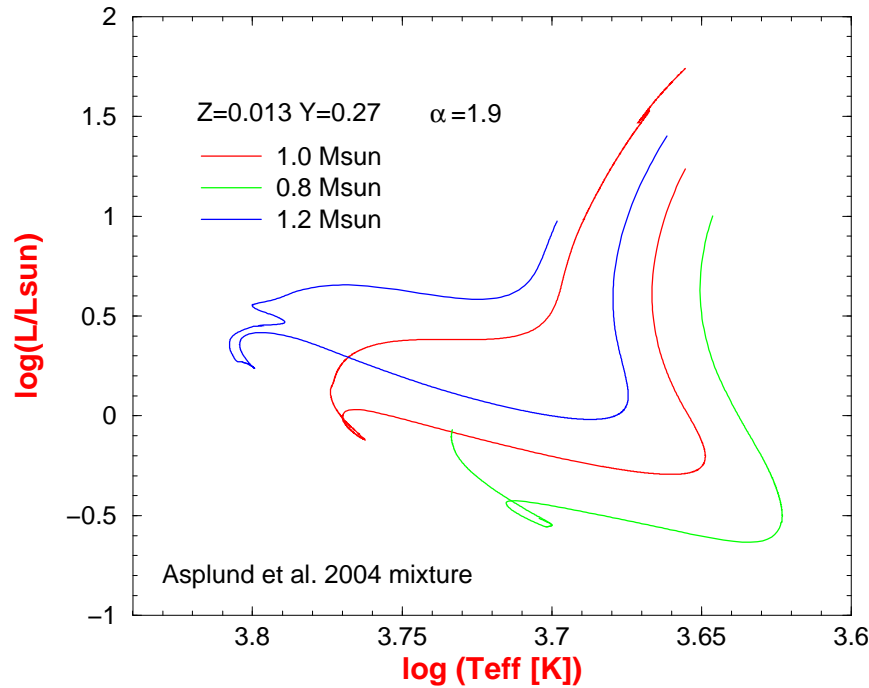


**Figure 6 :** Sestito, Degl'Innocenti, Prada Moroni, Randich 2006, *A&A* 454, 311

## Comparison with CESAM for TASK3 models Case 3.1

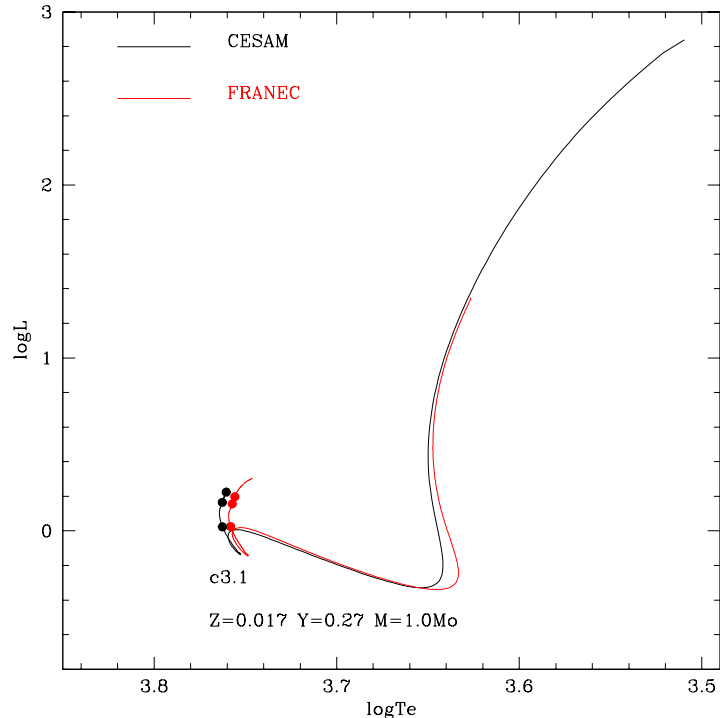


**Figure 7 :** Comparison of the positions in the HR diagrams of the selected models.

<i>mod</i>	<i>Age</i>	$R/R_\odot$	$L/L_\odot$	$T_{eff}$	$T_c/10^7$	$\rho_c$	$R_{env}/R$
	Gyr			K	K	$g/cm^3$	
3.1A	4.22	1.04	1.01	5666	1.57	153.95	0.7393
3.1B	7.28	1.22	1.37	5659	1.90	367.65	0.7275
3.1C	9.30	1.51	1.90	5527	1.93	1305.73	0.6752

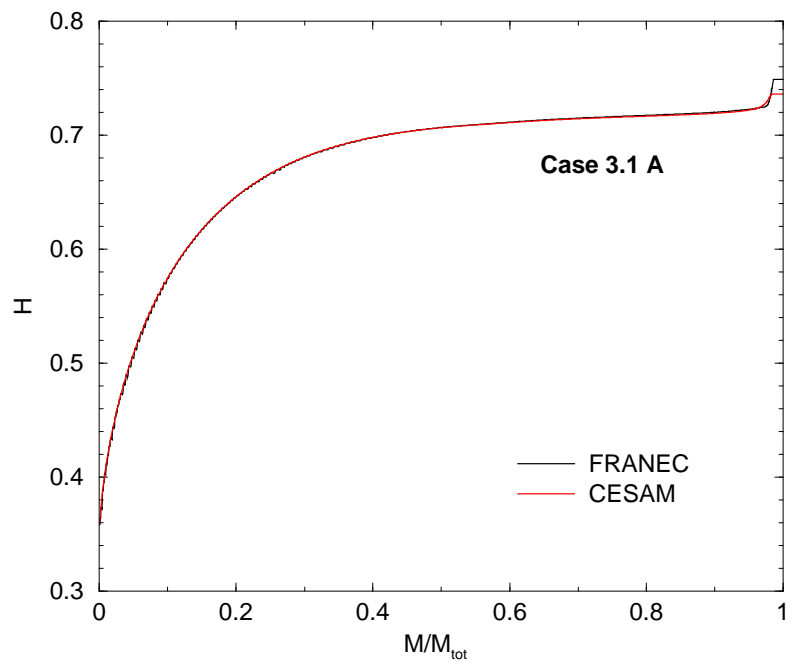


**Figure 8 :** Hydrogen abundance profile for model 3.1 A

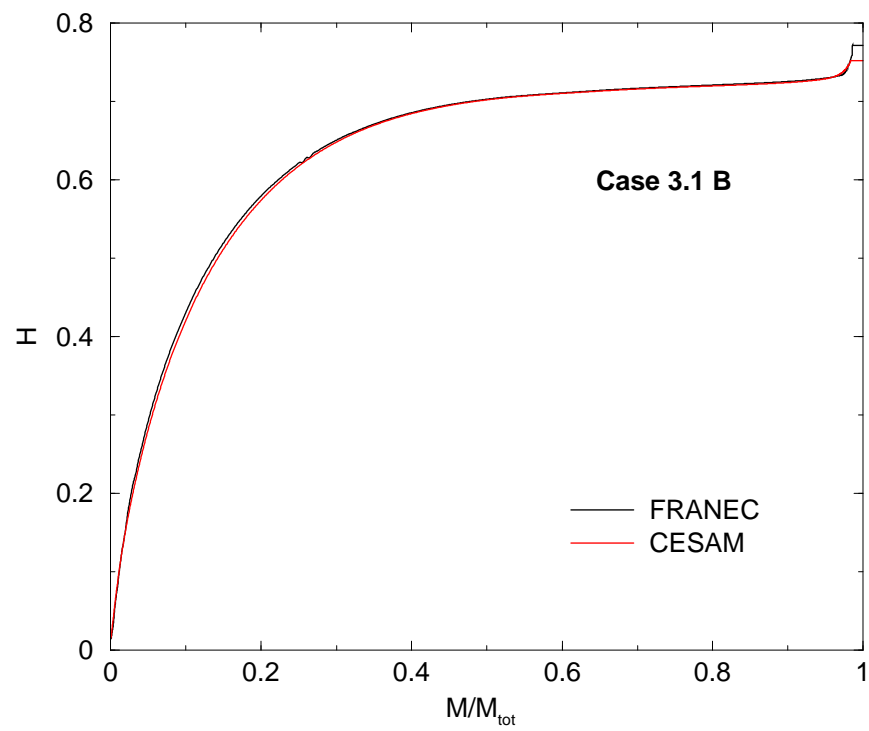


**Figure 9 :** Hydrogen abundance profile for model 3.1 B

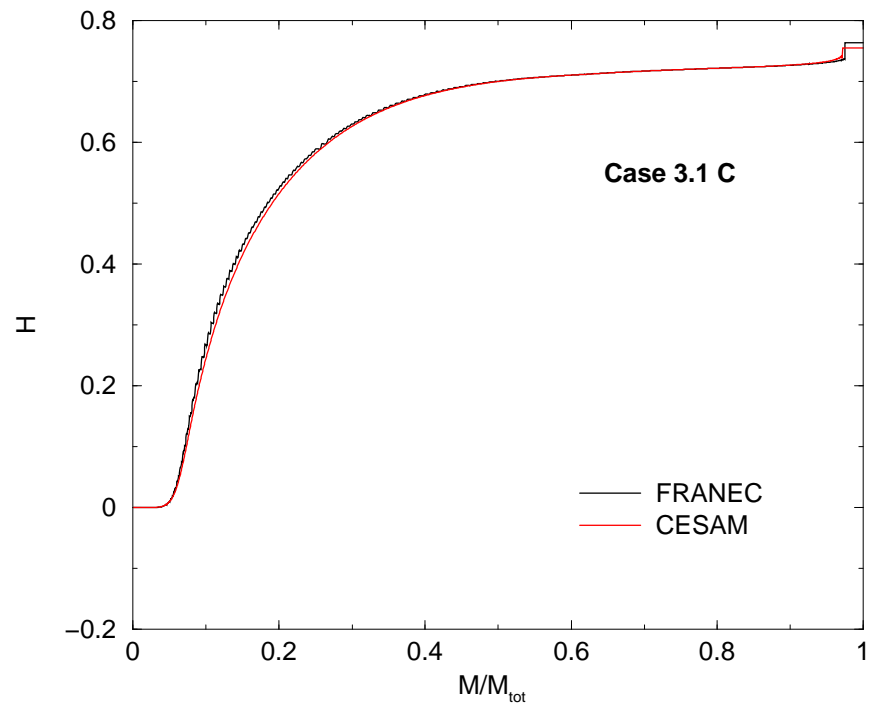


**Figure 10 :** *Hydrogen abundance profile for model 3.1 C*

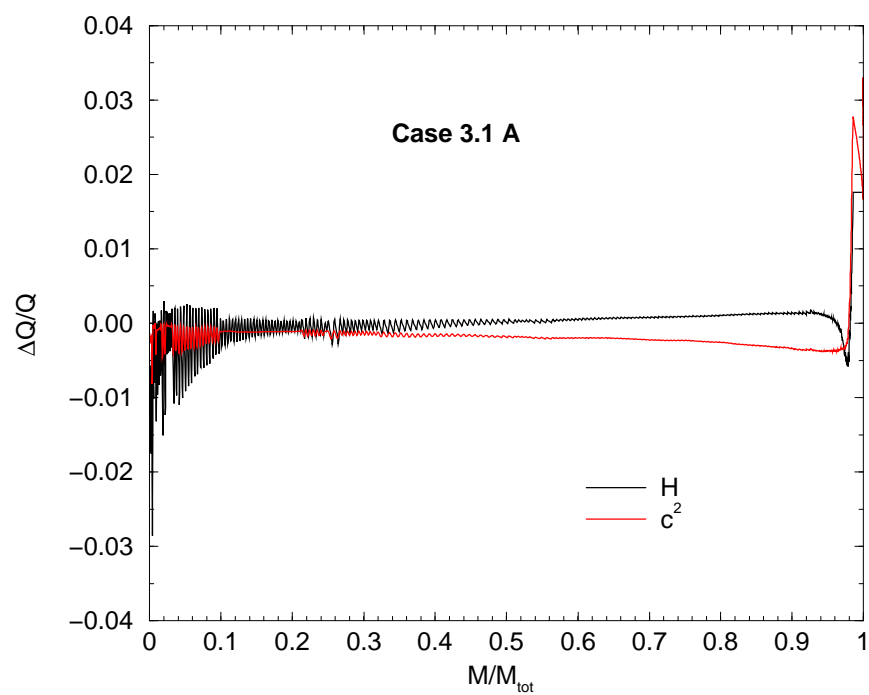


**Figure 11 :** *Relative difference in Hydrogen abundance and in the sound velocity value for model 3.1 A*

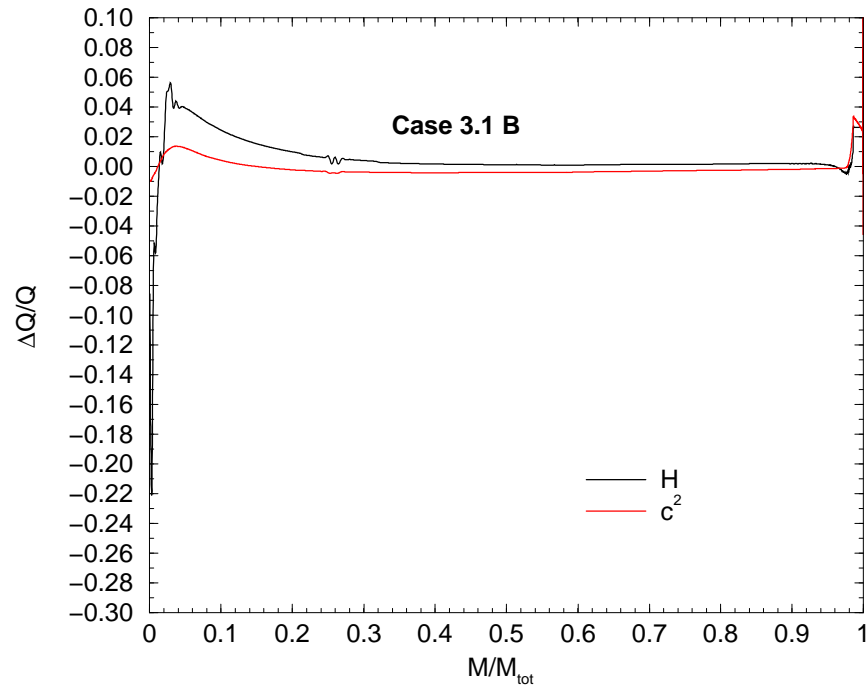


**Figure 12 :** *Relative difference in Hydrogen abundance and in the sound velocity value for model 3.1 B*

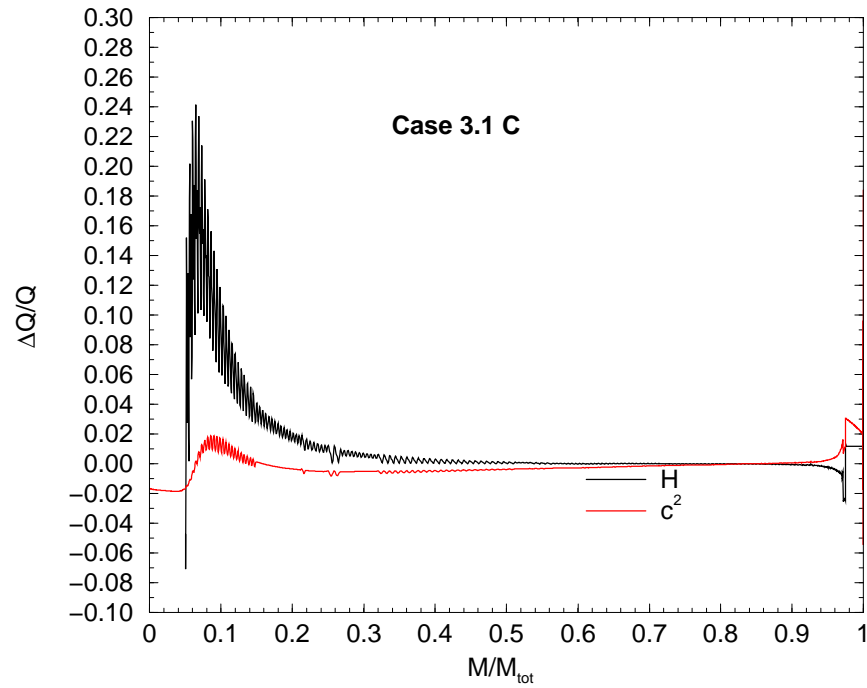


**Figure 13 :** *Relative difference in Hydrogen abundance and in the sound velocity value for model 3.1 C*

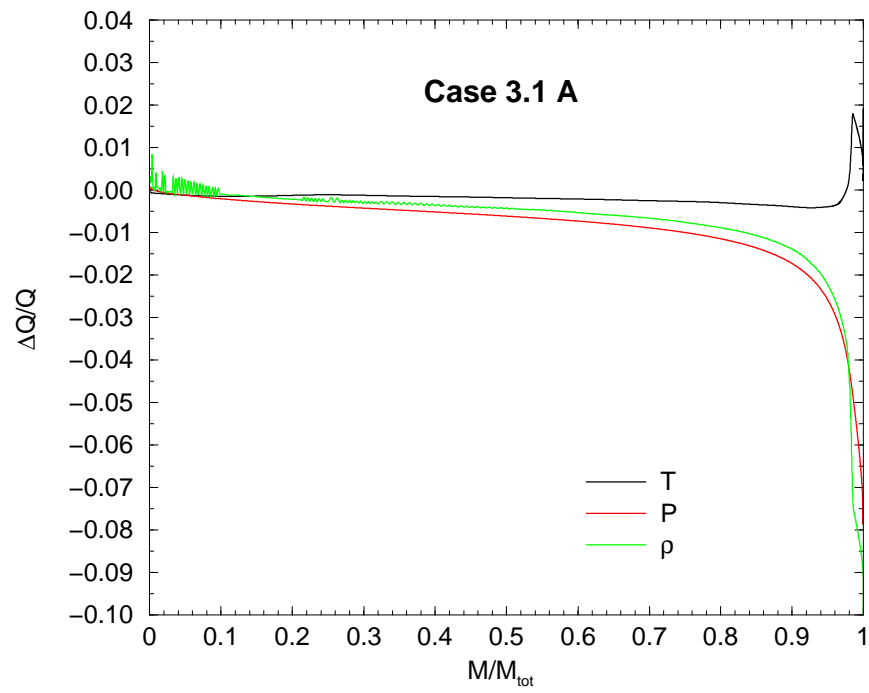


**Figure 14 :** Relative difference in  $P$ ,  $T$ ,  $\rho$  for model 3.1 A

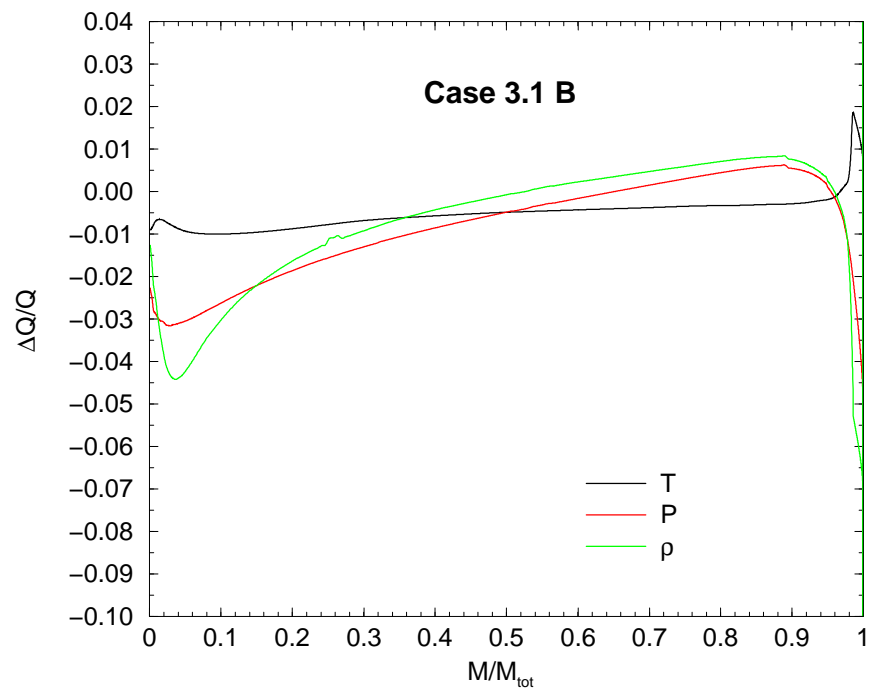


**Figure 15 :** Relative difference in  $P$ ,  $T$ ,  $\rho$  for model 3.1 B

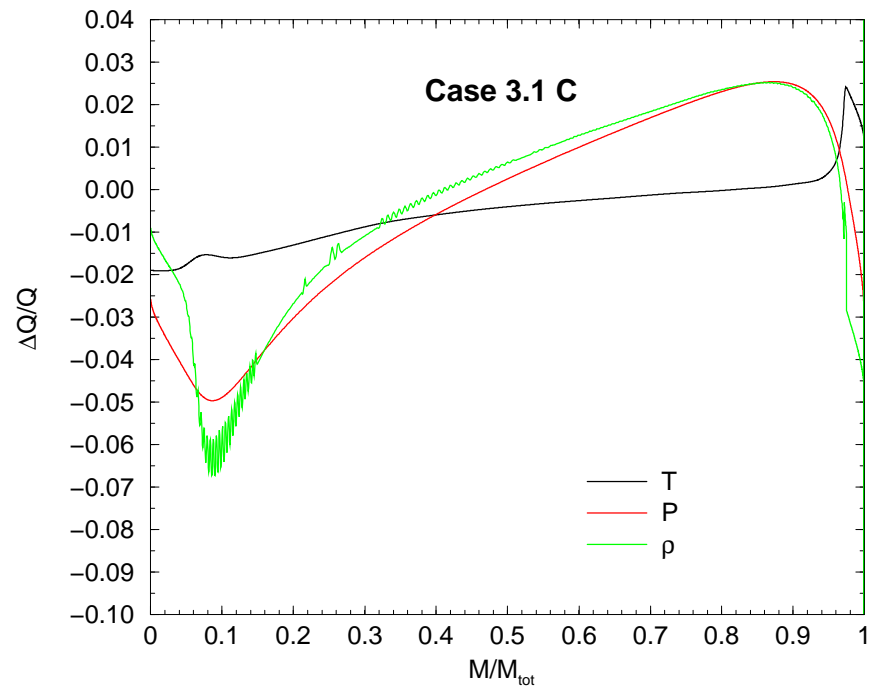


**Figure 16 :** Relative difference in  $P$ ,  $T$ ,  $\rho$  for model 3.1 C

## Comparison with CESAM for TASK3 models Case 3.2

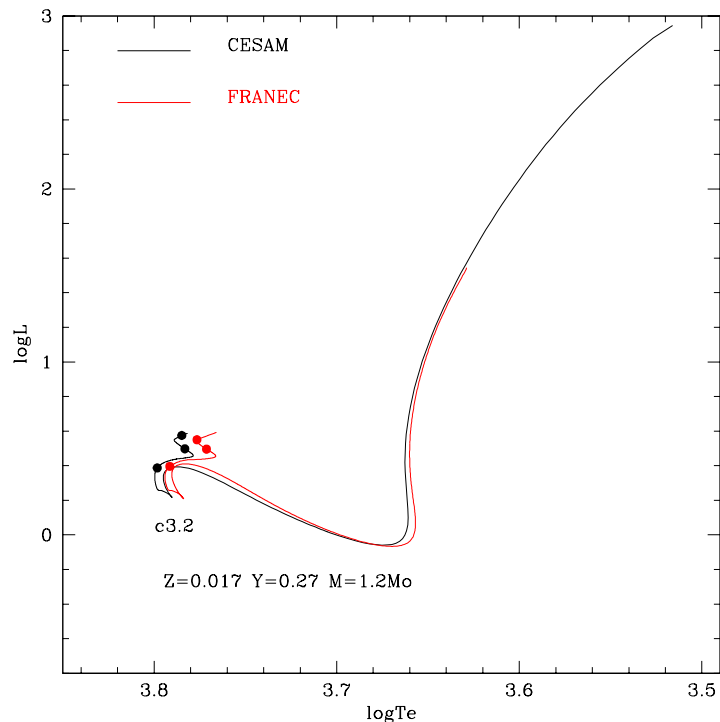


**Figure 17 :** Comparison of the positions in the HR diagrams of the selected models.

<i>mod</i>	<i>Age</i>	$R/R_\odot$	$L/L_\odot$	$T_{eff}$	$T_c/10^7$	$\rho_c$	$R_{env}/R$
	Gyr			K	K	$g/cm^3$	
3.2A	2.50	1.37	2.48	6203	1.86	142.60	0.8640
3.2B	4.22	1.69	3.12	5906	2.38	299.07	0.8192
3.2C	4.62	1.90	3.83	6203	2.00	1055.40	0.8108

## Case 3.2

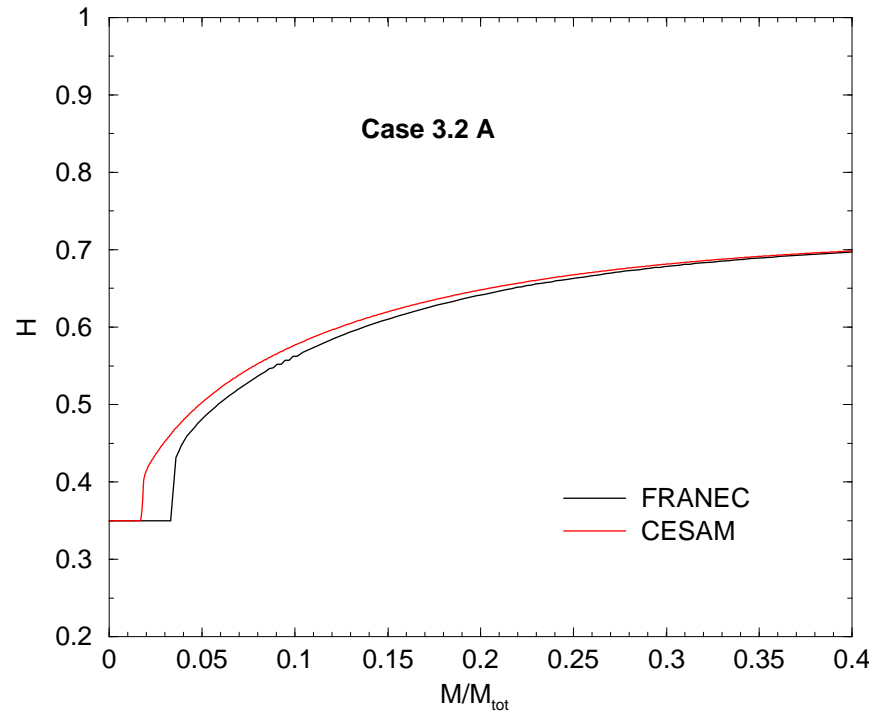


**Figure 18 :** Hydrogen abundance profile for model 3.2 A

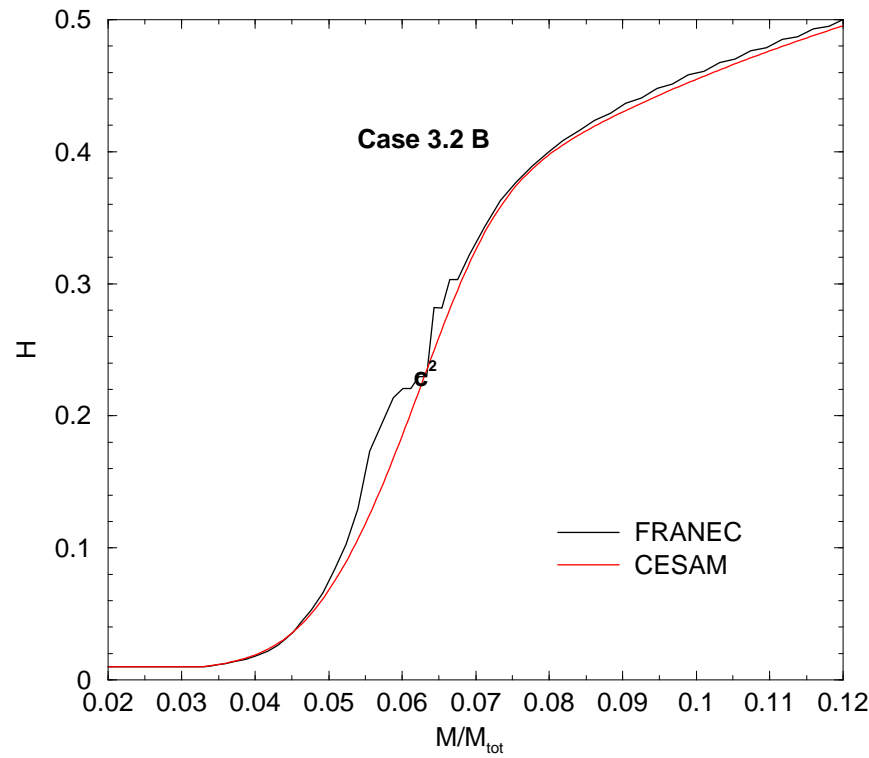


**Figure 19 :** Hydrogen abundance profile for model 3.2 B

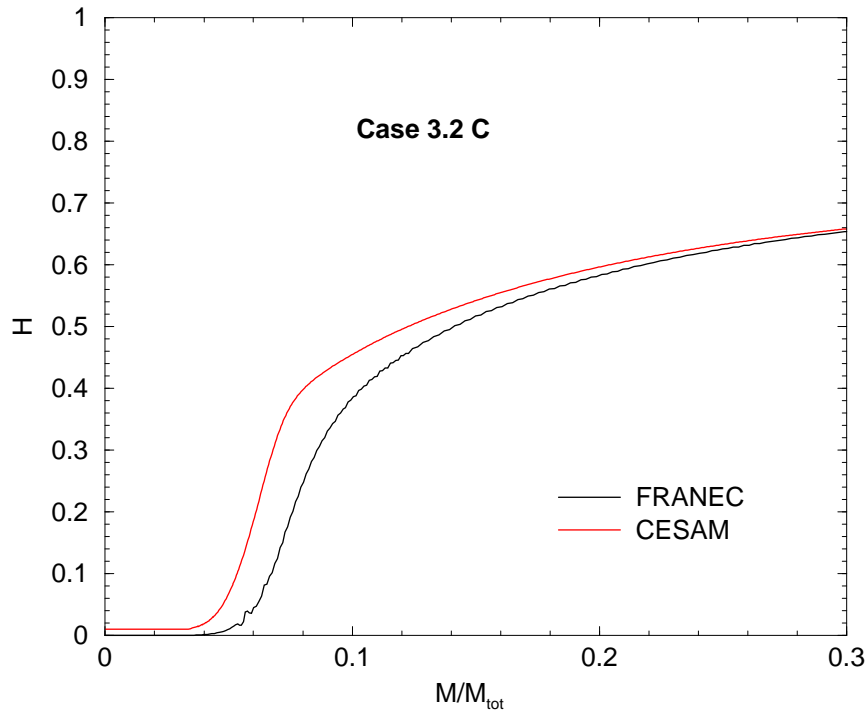


**Figure 20 :** *Hydrogen abundance profile for model 3.2 C*

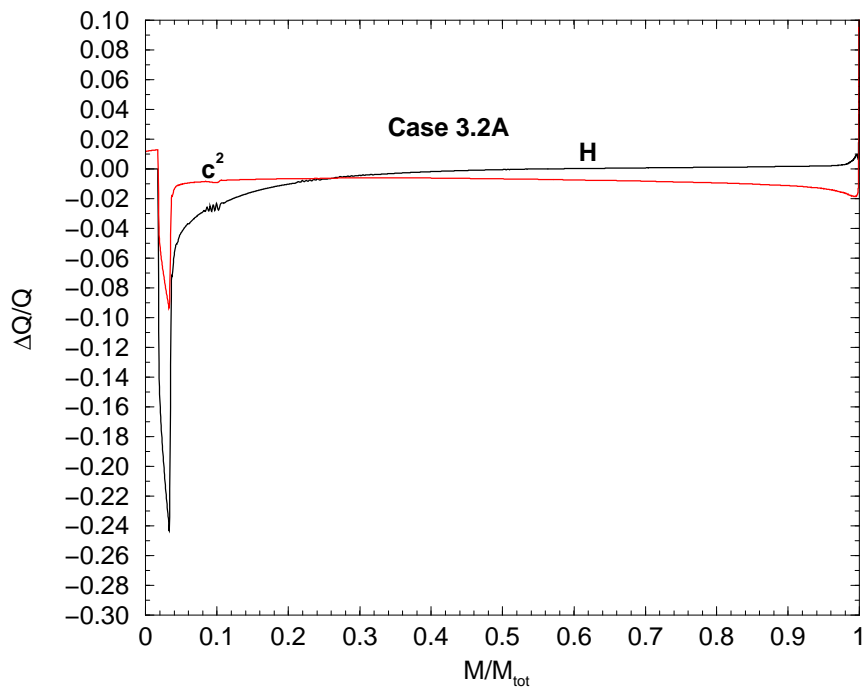


**Figure 21 :** *Relative difference in Hydrogen abundance and in the sound velocity value for model 3.2 A*

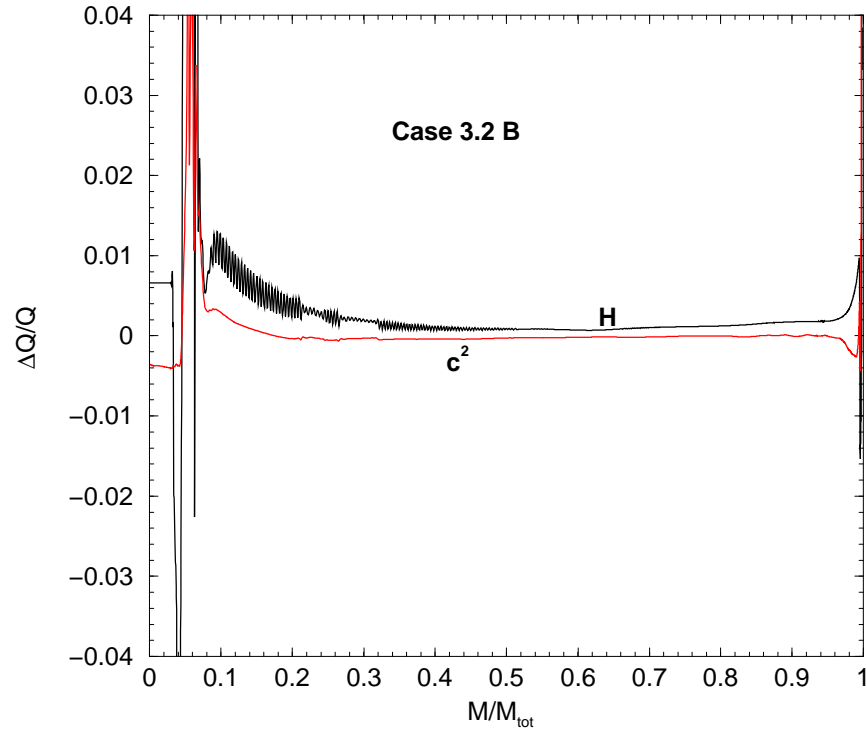


**Figure 22 :** *Relative difference in Hydrogen abundance and in the sound velocity value for model 3.2 B*

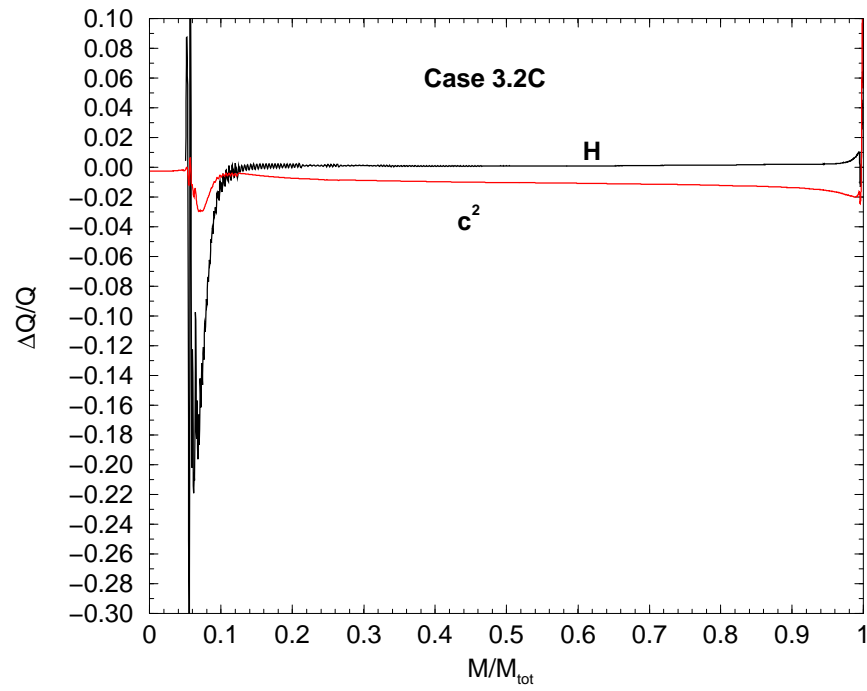


**Figure 23 :** *Relative difference in Hydrogen abundance and in the sound velocity value for model 3.2 C*

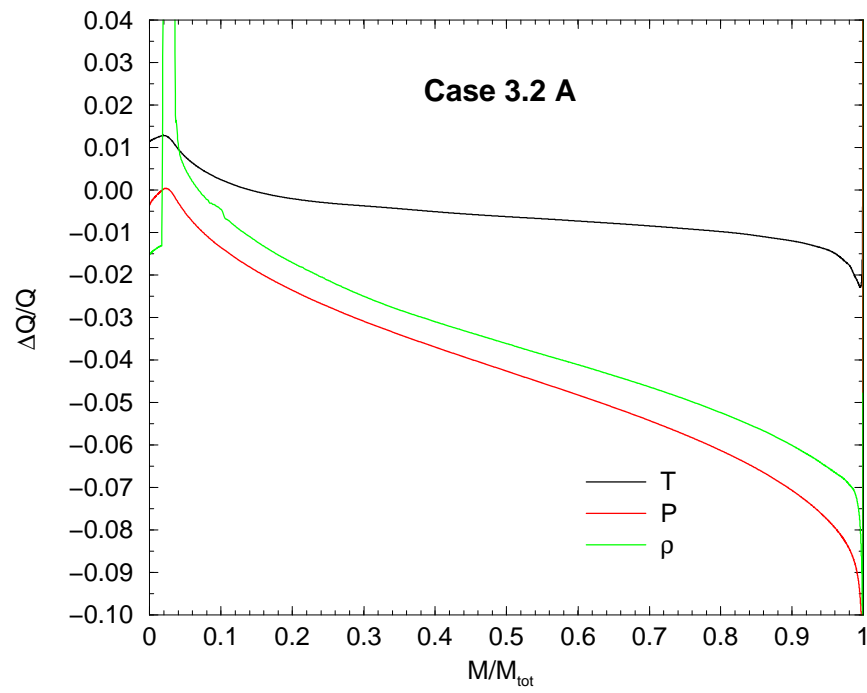


**Figure 24 :** Relative difference in  $P$ ,  $T$ ,  $\rho$  for model 3.2 A

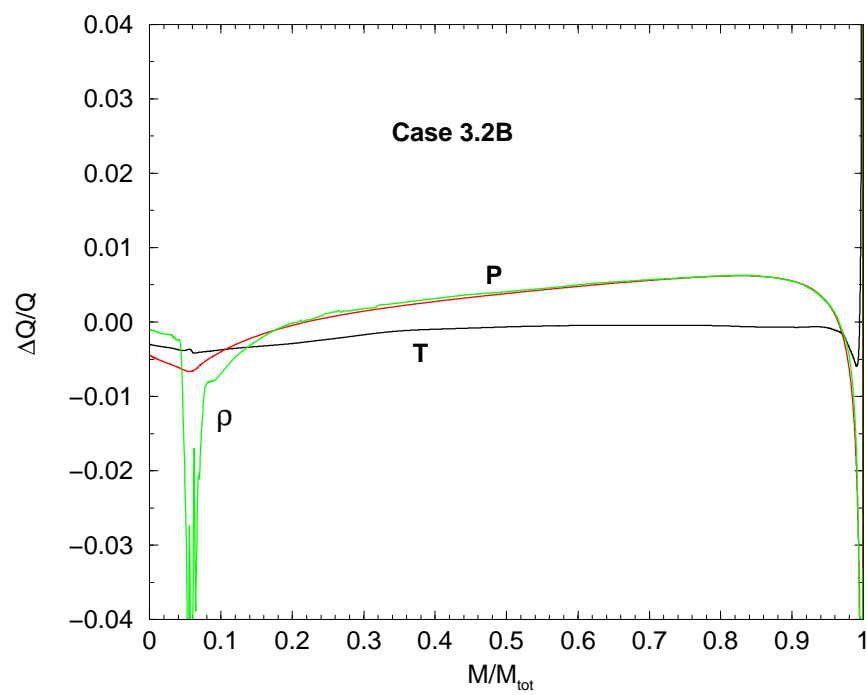


**Figure 25 :** Relative difference in  $P$ ,  $T$ ,  $\rho$  for model 3.2 B

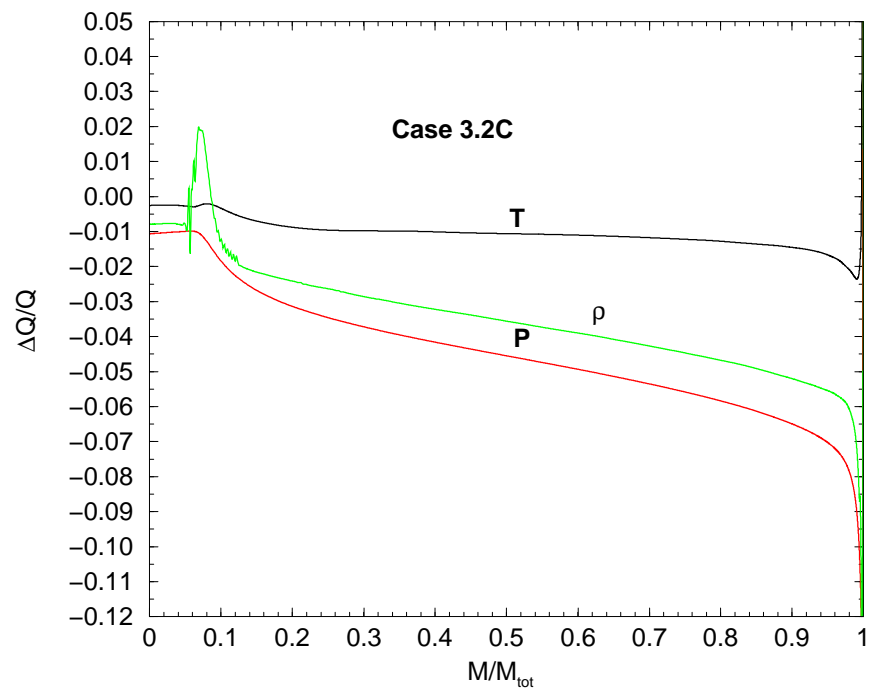


**Figure 26 :** Relative difference in  $P$ ,  $T$ ,  $\rho$  for model 3.2 C

## Comparison with CESAM for TASK3 models Case 3.3

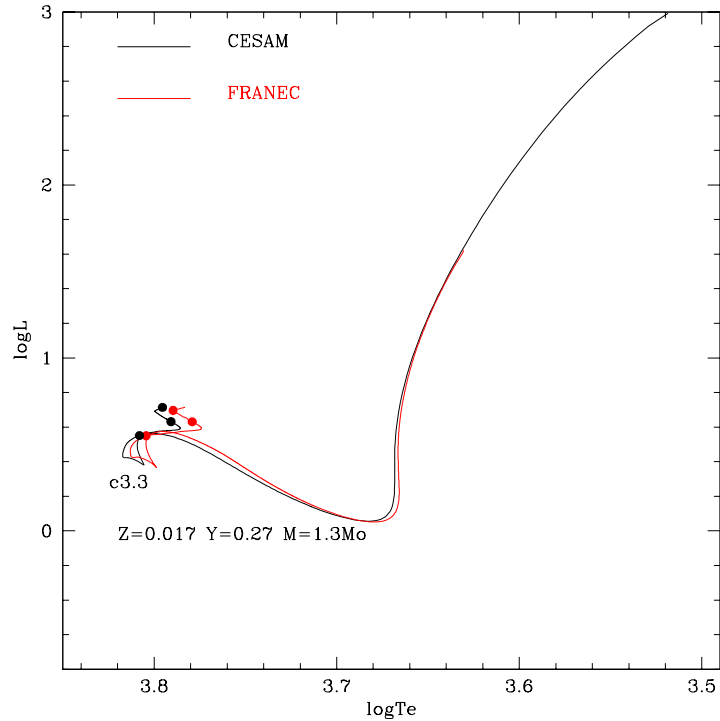


**Figure 27 :** Comparison of the positions in the HR diagrams of the selected models.

<i>mod</i>	<i>Age</i>	$R/R_\odot$	$L/L_\odot$	$T_{eff}$	$T_c/10^7$	$\rho_c$	$R_{env}/R$
	Gyr			K	K	$g/cm^3$	
3.3A	2.09	1.55	3.40	6304	1.97	129.78	0.0000
3.3B	3.25	1.90	4.09	5953	2.46	260.49	0.8455
3.3C	3.34	2.04	5.11	6081	2.04	945.20	0.8510

case 3.3

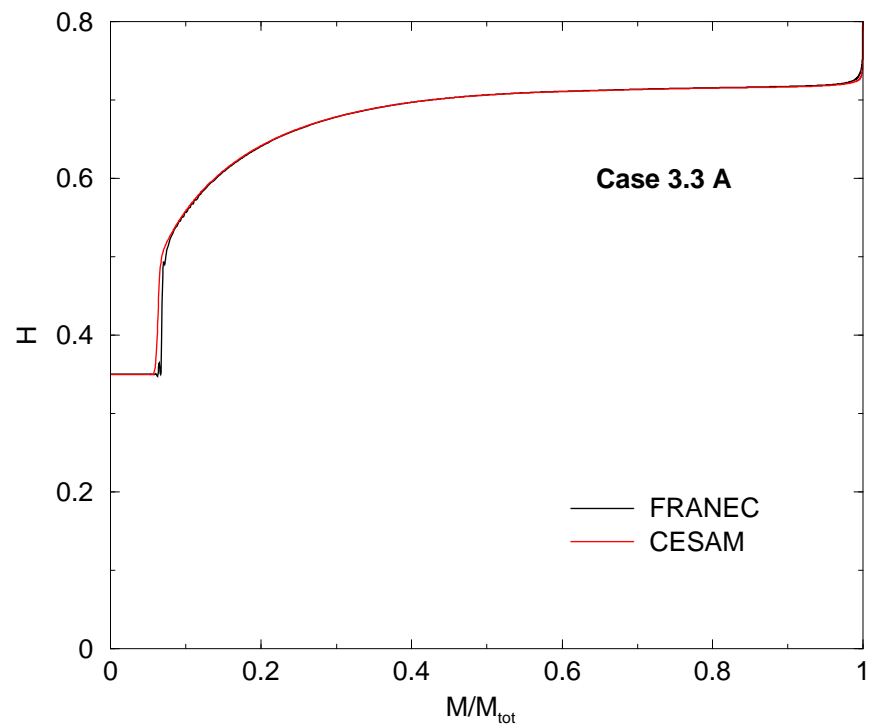


**Figure 28 :** Hydrogen abundance profile for model 3.3 A

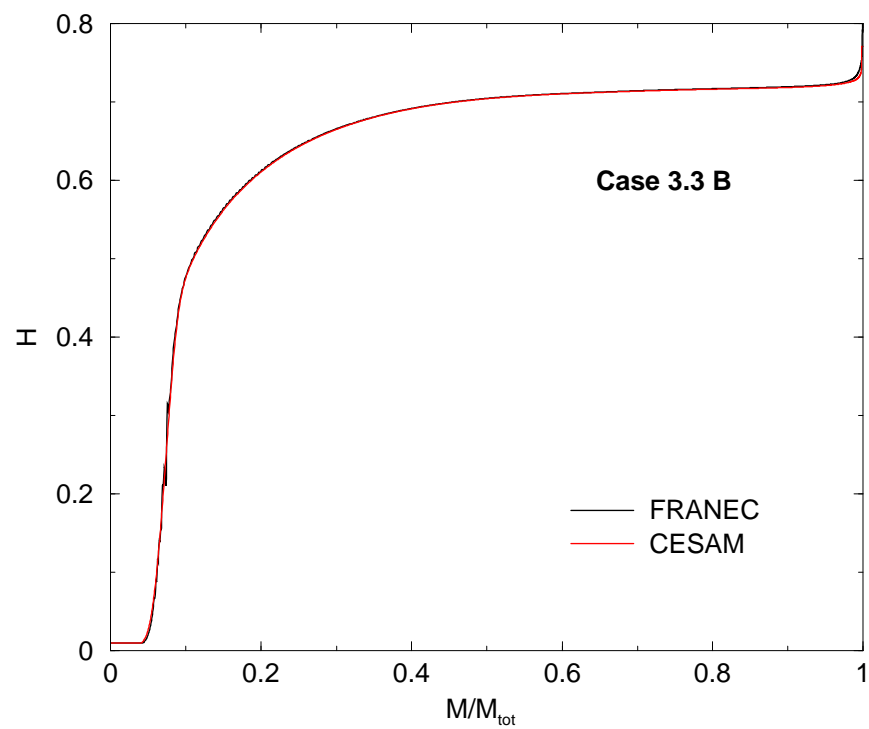


**Figure 29 :** Hydrogen abundance profile for model 3.3 B

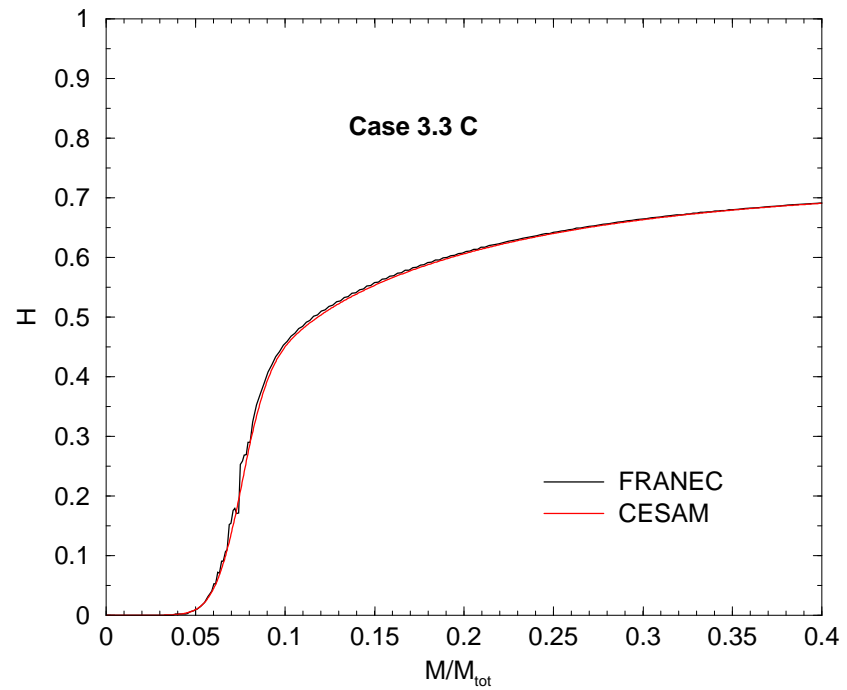


**Figure 30 :** Hydrogen abundance profile for model 3.3 C

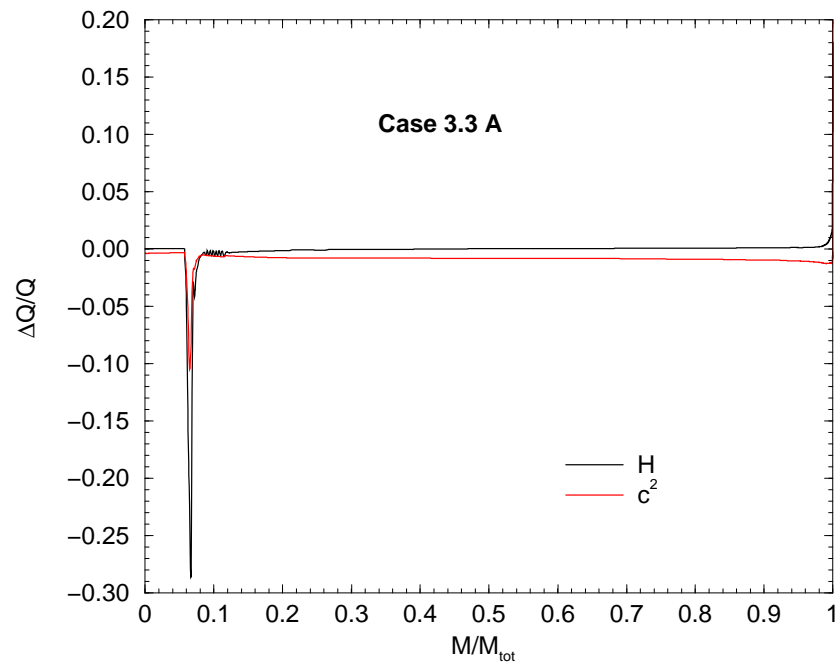


**Figure 31 :** *Relative difference in Hydrogen abundance and in the sound velocity value for model 3.3 A*

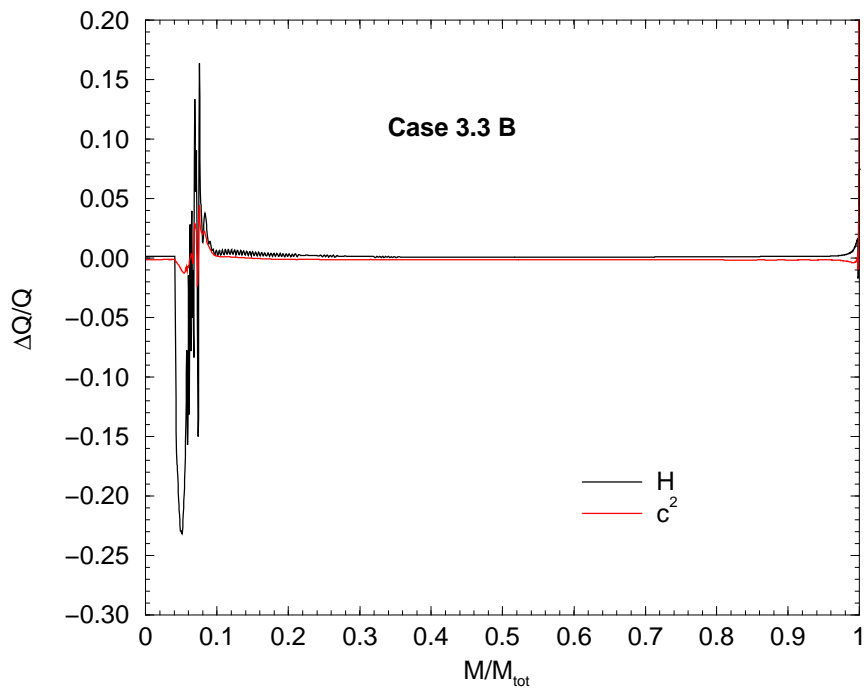


**Figure 32 :** *Relative difference in Hydrogen abundance and in the sound velocity value for model 3.3 B*

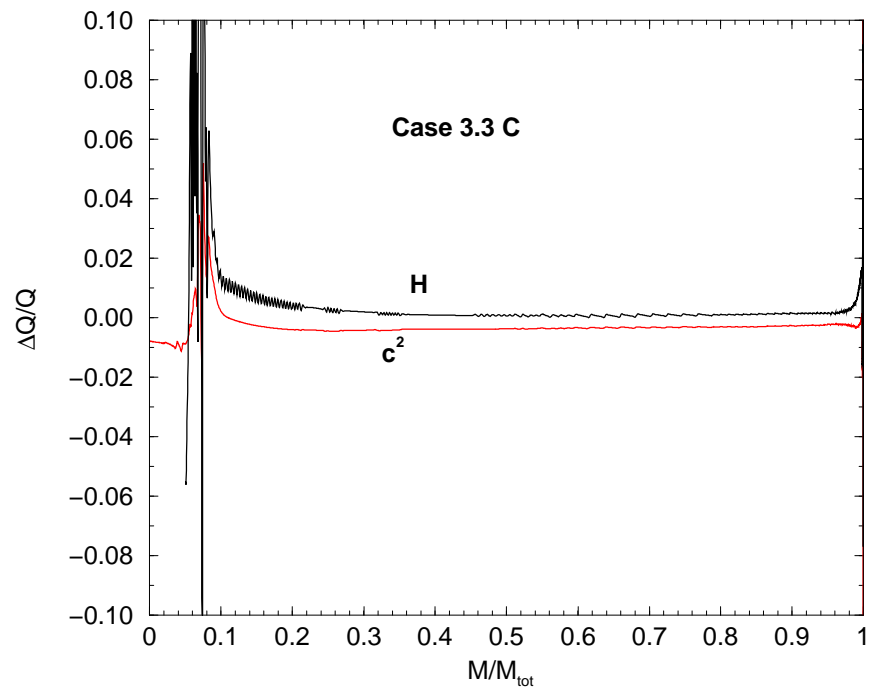


**Figure 33 :** Relative difference in Hydrogen abundance and in the sound velocity value for model 3.3 C

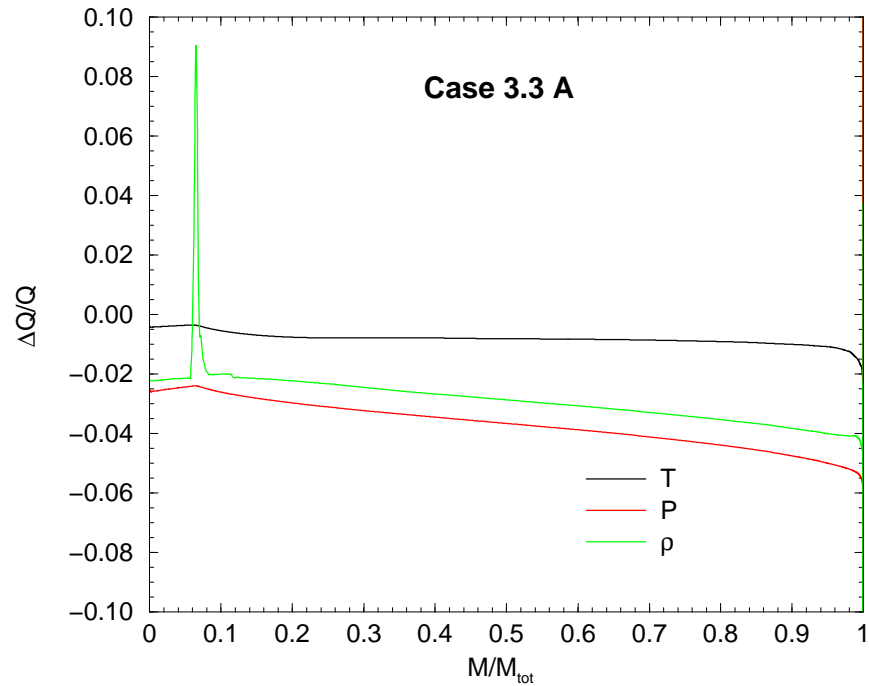


**Figure 34 :** Relative difference in  $P$ ,  $T$ ,  $\rho$  for model 3.3 A

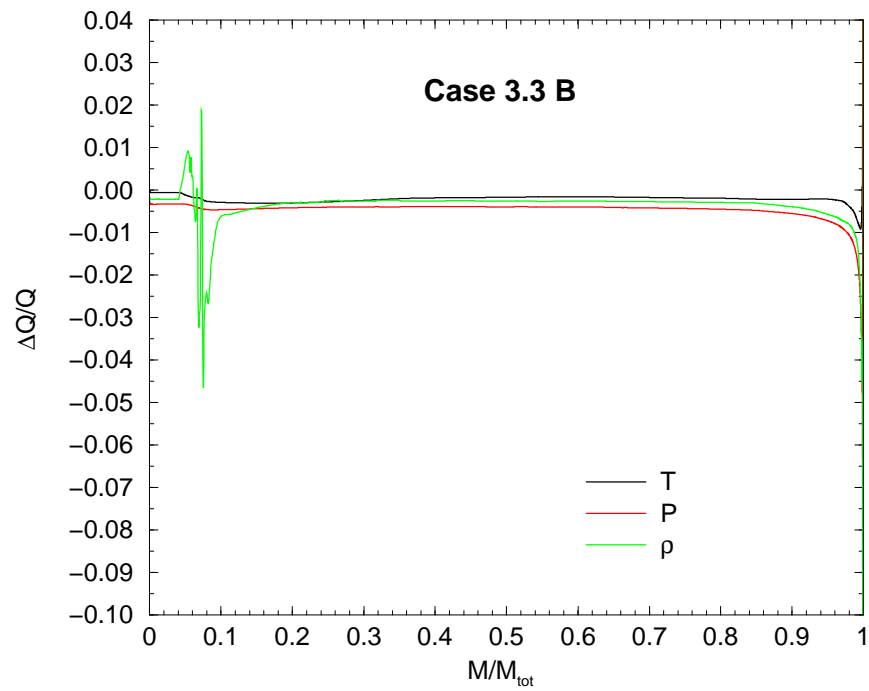


**Figure 35 :** Relative difference in  $P$ ,  $T$ ,  $\rho$  for model 3.3 B

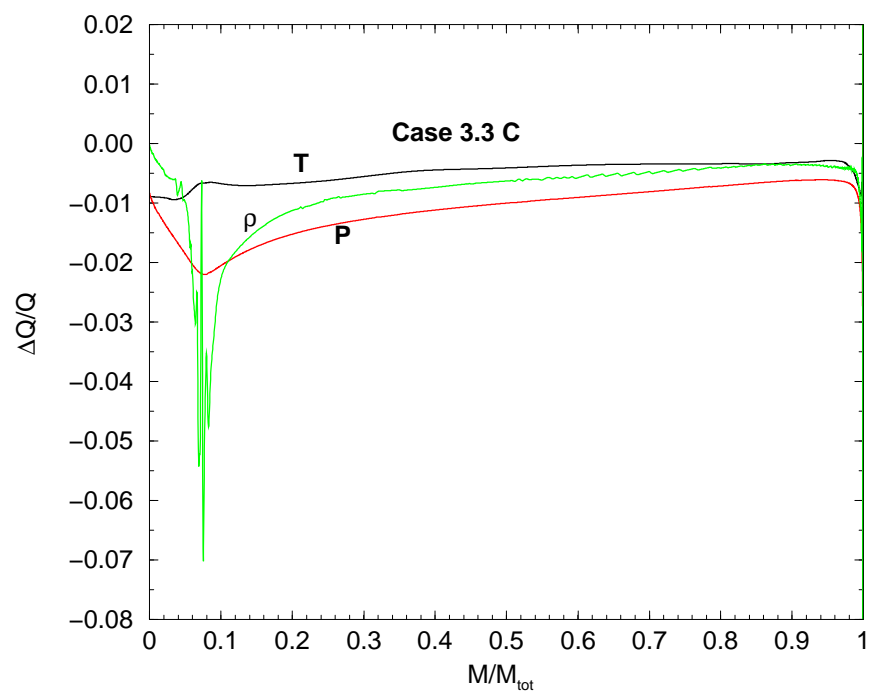


**Figure 36 :** Relative difference in  $P$ ,  $T$ ,  $\rho$  for model 3.3 C